A Lattice Boltzmann Model of Flow Blunting
Author(s): M. M. Dupin, I. Halliday and C. M. Care
Source: *Philosophical Transactions: Mathematical, Physical and Engineering Sciences*, Vol. 362, No. 1821, Connecting Scales: Micro, Meso and Macro Processes (Aug. 15, 2004), pp. 1755-1761
Published by: Royal Society
Stable URL: http://www.jstor.org/stable/4142378
Accessed: 24-08-2017 00:56 UTC

10.1098/rsta.2004.1403

THE ROYAL SOCIETY

A lattice Boltzmann model of flow blunting

BY M. M. DUPIN, I. HALLIDAY AND C. M. CARE

Materials Research Institute, Sheffield Hallam University, Howard Street, Sheffield S1 1WB, UK (mriih@exchange.shu.ac.uk)

Published online 3 June 2004

We review our recent multi-component lattice Boltzmann equation method for the simulation of a large number of mutually immiscible liquid species and then apply it to the simulation of dense volume fraction suspensions of deformable particles in internal geometry. In particular, we illustrate the scope of our method by applying it to the simulation of pipe flows containing a high volume fraction of monodisperse suspended, deformable particles. The particles are modelled as immiscible, relatively viscous liquid drops. We modify the 'solidity' of the particles by modifying their viscosity and surface tension and demonstrate the effect of the solidity upon the blunting of the velocity profile.

Keywords: lattice Boltzmann; multi-phase flow; blunting; particle solidity

1. Introduction

The lattice Boltzmann (LB) method shows real promise when applied to complex multi-component flow at low Reynolds number and a range of LB techniques have been developed to model fluid interfaces (e.g. Gunstensen *et al.* 1991; Thompson *et al.* 1999), with perhaps the Shan–Chen approach (Shan & Chen 1994) being the most popular. Here we consider two-dimensional simulations of mutually immiscible, and interacting, drops. The development of a method which is computationally efficient for $N \gg 2$ drops is a prime consideration of this work.

We base this work on an interfacial model, due originally to Gunstensen *et al.* (1991), with improved interface isotropy and reduced micro-current activity (Dupin *et al.* 2003). Where hydrodynamics alone defines a continuum case study, the Gunstensen interface algorithm is desirable, simply from the point of view of computational memory resources. From the many-component point of view, it provides a sharp interface necessary to obtain an efficient method in execution time and memory requirements, by reducing the number of nodes containing more than one colour (mixed nodes).

In § 2 *a*, we outline a binary model, with some recent improvements, and in § 2 *b*, we generalize to N immiscible fluids. In § 3, we consider how the 'solidity' of incompressible liquid drops, used to model a dense deformable particulate suspension, may be assessed by profile blunting (Dupin *et al.* 2004).

One contribution of 21 to a Theme 'Connecting scales: micro, meso and macro processes'.

2. General model

Our basic model is the two-dimensional nine-velocities (denoted D2Q9) weakly compressible LBGK (lattice Bhatnagar–Gross–Kross) model (Succi 2001), which has a single scalar collision parameter. In our multi-component version, segregation and surface tension are produced in any region of the lattice where colours mix by additional local (microscopic) rules. Such a region defines a fluid–fluid interface with essentially correct macroscopic (continuum-length-scale) properties (Thompson *et al.* 1999).

(*a*) *The two-phase model*

Since target flows are heavily interface dominated, the surface tension of our incompressible droplets is of prime consideration. It is activated by perturbing the post-collided densities $f_i(\boldsymbol{r}, t)$ of any mixed node as follows:

$$\Delta f_i(\boldsymbol{r}, t) = \lambda_i \sigma C(\boldsymbol{r}, t) \cos(2(\theta_f(\boldsymbol{r}) - \theta_i)), \tag{2.1}$$

where λ_i is a modulation parameter ensuring good isotropy of the interface and reduced micro-current flow (see Dupin *et al.* (2003) for more details). λ_i takes a value of $\sqrt{3}/2$ for the short links and unity for the long links (cf. the D2Q9 model). C is a concentration factor which limits activation of surface tension to multicoloured nodes. θ_f is the direction of the local colour gradient, being the normal to the local interface as a good approximation. θ_i is the direction of the ith link.

Colour segregation is ensured by numerically reallocating colour in the colour-blind post-collided f_i so as to maximize the work done by the colour flux against the colour gradient (Gunstensen *et al.* 1991).

(*b*) *The N-phase model*

We now consider the generalization of the diphasic model in (§ 2 *a*) to a mixture of N immiscible liquids in which mutual coalescence and evaporation is completely suppressed.

Our generalization to N immiscible components assigns each fluid a 'colour' superscript, $\Gamma = 0, 1, 2, 3, \ldots, (N-1)$. Fluids with different values of Γ can have different properties, e.g. collision parameters τ_Γ and, accordingly, viscosity ν_Γ. Now, for N different species, multi-component LB quickly demands impractical amounts of computer storage, as N increases. However, for non-evaporating fluids forming 'sharp' interface drops the arrays for N hydrodynamic quantities $(f_i^\Gamma(\boldsymbol{r}, t),\ \rho^\alpha(\boldsymbol{r}, t))$, are very sparse, hence the use of the Gunstensen-type interface.

Consequently, to minimize storage, we record only N_c, with $N_\mathrm{c} < Q \ll N$, species at any node, which gives considerable reduction in the required storage. The sharp interfaces from our Gunstensen-type interface method mean minimal mixing and a reduction in the number of different colours found on a node, as well as a reduction in the total number of mixed nodes. In practice we take $N_\mathrm{c} = 5$. This value is found to be adequate for even the most intimately monodisperse multi-component flows. Note, however, that the number of colours, or immiscible components, varies between nodes and in time.

In our generalization to N different fluids, we assign each local hydrodynamic density $(f_i(\boldsymbol{r}, t))$ a superscript α $(0 \leqslant \alpha < N_\mathrm{c})$, which is used to identify the fluids

associated with the node. Clearly, the identification of particular fluids within a node must refer to the lattice map of absolute colour, $l(\boldsymbol{r}, i, \alpha)$. However, for such a map sufficient information can be stored in a four-dimensional array of integer type. Both l and the hydrodynamic densities f now have a subscript set $\{x, y, i, \alpha\}$ to identify, for lattice position $\{x, y\}$, direction i, the colours present at the node. We note that these two quantities propagate jointly along the lattice.

By recording at most N_c species at each node, the storage and time requirements are reduced by a factor N_c/N, to levels comparable with the diphasic model (see § 2 *a*).

In the N-phase model, as in the diphasic model, collision is performed in three steps: mixed fluid collision, perturbation and colour reallocation. The collision of the mixed fluid's momentum densities,

$$f_i(\boldsymbol{r}, t) = \sum_{\alpha=0}^{N_c-1} f_i^{\alpha}(\boldsymbol{r}, t), \tag{2.2}$$

is performed on the mixed fluid, exactly after Zou *et al.* (1995), with an effective relaxation parameter giving, at a mixed node, the effective viscosity

$$\nu(\boldsymbol{r}, t) = \frac{1}{\rho(\boldsymbol{r}, t)} \sum_{\alpha=0}^{N_c-1} \rho^{\alpha}(\boldsymbol{r}, t)\nu^{\alpha},$$

where ν_α defines the chosen kinematic viscosity of any component α present at $\boldsymbol{r}$ which relates to a particular ν^{Γ} through the colour map $l(\boldsymbol{r}, i, \alpha)$, and

$$\rho(\boldsymbol{r}, t) = \sum_{\alpha=0}^{N_c-1} \rho^{\alpha}(\boldsymbol{r}, t), \qquad \rho^{\alpha}(\boldsymbol{r}, t) = \sum_{i=0}^{Q-1} f_i^{\alpha}(\boldsymbol{r}, t).$$

Controlling coalescence amounts to dealing consistently with all possible colour pairs at every mixed node, in order to eliminate any mixing between species after propagation. This requirement may still be stated as a need to maximize the work done by a generalized colour flux against a generalized colour gradient (following Gunstensen *et al.* 1991). Accordingly, the diphasic colour gradient is generalized to any pair of fluids α and β at a node.

We may define a colour gradient at the interface between fluid α and fluid β by what we assume to be its local normal:

$$\boldsymbol{I}_{\alpha\beta}(\boldsymbol{r}) = \sum_i (\rho^{\alpha}(\boldsymbol{r} + \boldsymbol{c}_i) - \rho^{\beta}(\boldsymbol{r} + \boldsymbol{c}_i))\boldsymbol{c}_i. \tag{2.3}$$

This colour gradient is used to perturb the mixed fluid's momentum densities (equation (2.2)). For the interface between two components α and β we use a generalized perturbation after equations (2.1):

$$\Delta f_i(\boldsymbol{r}, t) = \sum_{(\alpha,\beta)} \Delta f_i^{\alpha,\beta}(\boldsymbol{r}, t) = \sum_{(\alpha,\beta)} \sigma_{\alpha\beta}\lambda_i C_{\alpha\beta}(\boldsymbol{r}, t) cos(2(\theta_f(\boldsymbol{r}) - \theta_i)), \tag{2.4}$$

in which there is no summation on repeated subscripts, but the summation is taken on all possible pairs α, β. $\sigma_{\alpha\beta}$ is a surface tension parameter for the interface between

fluid α and fluid β and

$$C_{\alpha\beta}(\boldsymbol{r},t) = 1 - \left|\frac{\rho_\alpha(\boldsymbol{r},t) - \rho_\beta(\boldsymbol{r},t)}{\rho_\alpha(\boldsymbol{r},t) + \rho_\beta(\boldsymbol{r},t)}\right| \tag{2.5}$$

is the concentration factor for the α, β fluid pair, after the diphasic model of § 2 *a*. λ_i is the modulating factor introduced in § 2 *a*. We now define an 'average' colour gradient which points towards component α and away from the total of all other components present at the node at position $\boldsymbol{r}$:

$$\boldsymbol{f}^\alpha(\boldsymbol{r}) = \sum_i [2\rho^\alpha(\boldsymbol{r}+\boldsymbol{c}_i) - \rho(\boldsymbol{r}+\boldsymbol{c}_i)]\boldsymbol{c}_i. \tag{2.6}$$

The same calculations ((2.4) and (2.5)) are repeated for each pair of fluid components α, β present at the node, position $\boldsymbol{r}$. To avoid coalescence, the appropriate colour gradient $\boldsymbol{f}^\alpha(\boldsymbol{r})$ (equation (2.6)) is used to recolour component α within each node, essentially in the same way as for a binary fluid but with the order in which components α are treated being significant. Note that to calculate the colour gradient (2.6) requires knowledge of the absolute colour, not just the relative amounts of the different colours present in a local environment.

It is crucial to note that we have shown that execution time and memory requirements scale linearly with the simulation size (total number of nodes) and N_c but are almost independent of N (Dupin *et al.* 2003).

3. Simulations

As an initial step, to avoid the need to postulate sublattice lubrication forces associated with thin layers of fluid, we manipulate wetting to ensure that a resolved layer of ambient liquid always remains between drops and any boundary. We therefore need to ensure preferential wetting of the boundary and suspended drops by the ambient fluid. This was achieved for the simulations here in the manner described in Dupin *et al.* (2003). The correct hydrodynamics recovered in Dupin *et al.* (2004) (also depicted in §§ 3 *a* and 3 *b*) tend to support this assumption for a volume fraction of particle, Φ, up to 0.6 at least. Targeted flows are, by intention, heavily interface dominated. We investigate the blunting of the flow profile, β (see below), of a suspension of N particles at a volume fraction Φ of viscosity ratio (droplets/surrounding) Λ, surface tension σ, in a straight channel. We employed the well-established mid-link bounce-back method (Succi 2001) top and bottom. Periodic boundary conditions were applied left and right. The flow rate is quantified by the pressure gradient ΔP/length along the channel. By inspection, our blunted profiles have noticeable departure from parabolic profiles. We measure averaged departure, at normalized cross-duct distance $\bar{y} = 0.25$ and $\bar{y} = 0.75$, by defining the blunting β:

$$\beta \equiv \frac{\bar{v}(\bar{y}=0.25) + \bar{v}(\bar{y}=0.75)}{2 \times 0.75}, \tag{3.1}$$

in which 0.75 is the height of a normalized parabola. With this definition, a flat velocity profile is characterized by $\beta = 1.33$ and a parabolic velocity profile by $\beta = 1.00$.

(*a*) *Rigid particles*

It has been found experimentally that for rigid suspended particles, the velocity profile is determined *solely* by the suspension concentration and the relative particle size (Caro *et al.* 1998). We considered that immiscible incompressible drops with $\Lambda = 50$ and high surface tension represented solid particles over that range of flow rates (specified by ΔP) for which the expected invariance in bulk flow parameter β was observed. Note, however, that, by increasing ΔP without bound, small changes in β occur (Dupin *et al.* 2004), showing the limits of the solid-particle behaviour of our droplets at high forcing.

(*b*) *Flexible particles*

For immiscible liquid drops (i.e. flexible particle suspensions) with $\Lambda = 1$ and smaller σ on the other hand, we observed the expected decrease of β upon increasing ΔP (Dupin *et al.* 2004; Caro *et al.* 1998).

(*c*) *Simulation results: rigid or flexible particles?*

It is appropriate to test our method by using it to resolve the changes that occur between deformable- and solid-particle-based bulk suspension behaviour, using parameters Λ and σ. We consider dense suspensions $\Phi = 0.6$ in order to ensure $\beta \to 1.33$ (solid-particle bulk behaviour, § 3 *a* above). With large Λ and σ, we limit ΔP to lie within the constant-β 'solid-particle' regime (§ 3 *a*). For small Λ and σ, the choice of ΔP should allow $\beta \to 1.00$ (deformable suspension bulk behaviour) to be observable (§ 3 *b*). Figure 1 shows the contours of the departure of β from a parabola as a function of Λ and σ. The data of this figure were compiled using the method outlined at the start of this section.

The simulation size was 250×100, the ambient fluid had a relaxation parameter $\omega = 1.7$, and the particle relaxation parameter varied between 0.1 and 1.9 in increments of 0.2 (giving viscosity ratios from 0.3 to 110). The surface tension varied (14 different values) from its maximum value (giving stable simulations in this configuration with $\sigma \leqslant 0.006$) down by three orders of magnitude. Values of β were calculated at steady state, typically after 5×10^5 iterations. The surface is an interpolation of the fitted measurements. The measured values of β departed typically from this interpolated surface by 10% (standard deviation from the data and the interpolated curve). This scattering is due to the noise on the measured velocity profile, from which β is extracted.

As we saw previously, one can relate blunting dependence to solidity. With the set of parameters of figure 1, it provides a calibration of the 'solidity' of the suspended particles upon parameters σ and Λ (through the measured value of β). In terms of elaborating a possible empirical rule, it is interesting to note that curves of β as a function of Λ, parametrized by σ, appear to be self-similar. The curves are similar in turn to self-similar curves of β as a function of σ, parametrized by Λ. It is worth noticing that figure 1 confirms the droplet behaviour that one would expect: the droplet's 'solidity' (here measured by β) increases with increasing viscosity ratio (Λ) and with increasing droplet surface tension (σ).

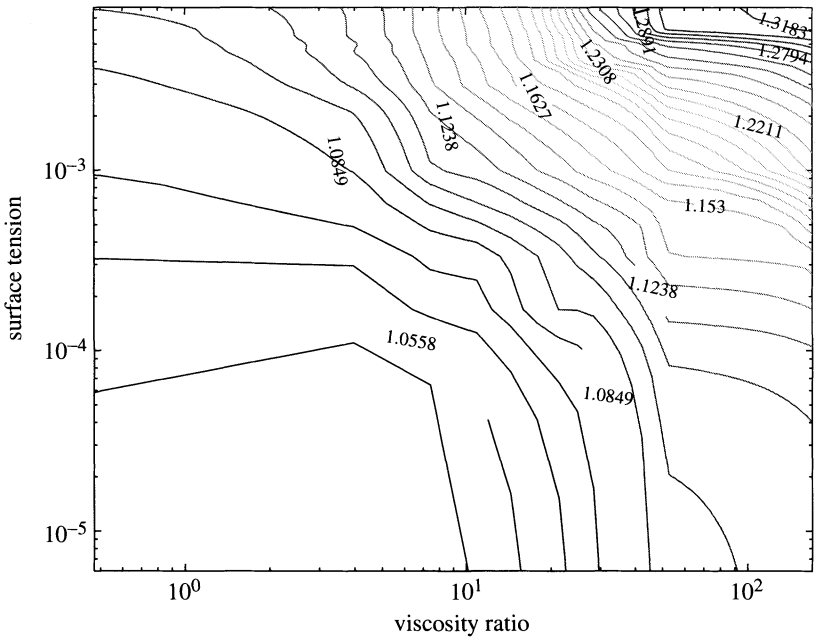

Figure 1. Blunting β contours for the flow of droplets in suspension as a function of their surface tension and viscosity (the surface from which these contours have been taken is an interpolation of the values of β calculated from fitted velocity profiles). The pure parabolic profile corresponds to $\beta = 1.0$ and the plug flat profile to $\beta = 1.33$.

4. Conclusion

In conclusion, we have demonstrated a model for large numbers of non-coalescing, non-evaporating, mutually immiscible incompressible liquid drops. From the results here (figure 1), the model supports a large range of parametrization, e.g. ambient fluid to drop viscosity ratio and surface tensions, and is able to recover correct bulk 'macroscopic' flows from the particular set of microscopic rules in use. This observation is particularly relevant as a vindication of our representation of lubrication forces. With the help of this new lattice Boltzmann scheme, we have been able to *microscopically* parametrize dense suspensions of immiscible drops by relative viscosity and surface tension to produce *macroscopic* effects on bulk channel flows which, qualitatively at least, encompass the range of behaviour from solid suspensions to suspensions of deformable particles. In addition to the latter, this calibration provides crucial information for future investigations where one might need to model solid particles at a given flow rate. This opens unique possibilities for investigation, where deformability cannot be ignored when simulating advecting suspensions.

Where particle deformation is high, one might expect close contacts between drops at high volume fraction. Accordingly, the representation of sublattice lubrication forces in the algorithm is the first point at which work needs to be undertaken.

References

Caro, C. G., Pedeley, T. J., Schroter, R. C. & Seed, W. A. 1998 *The mechanics of the circulation.* Oxford Medical Publications.

Dupin, M. M., Halliday, I. & Care, C. M. 2003 Multi-component lattice Boltzmann equation for mesoscale blood flow. *J. Phys.* A **36**, 8517–8534.

Dupin, M. M., Halliday, I. & Care, C. M. 2004 Multi-component lattice Boltzmann equation. (Submitted.)

Gunstensen, A. K., Rothman, D. H., Zaleski, S. & Zanetti, G. 1991 Lattice Boltzmann model of immiscible fluids. *Phys. Rev.* A **43**, 4320–4327.

Shan, X. W. & Chen, H. D. 1994 Simulation of non-ideal gases and liquid–gas phase transitions by the lattice Boltzmann equation. *Phys. Rev.* E **49**(4), 2941–2948.

Succi, S. 2001 *The lattice Boltzmann equation.* Oxford: Clarendon.

Thompson, S. P., Halliday, I. & Care, C. M. 1999 Mesoscopic hydrodynamics of diphasic lattice Bhatnagar–Gross–Krook fluid interfaces. *Phys. Chem. Chem. Phys.* **1**, 2183–2190.

Zou, Q., Hou, S., Chen, S. & Doolen, G. D. 1995 Analytical solutions of the lattice Boltzmann BGK model. *J. Stat. Phys.* **81**, 319–334.